Odorized and deodorized aqueous extracts of *Ammodaucus leucotrichus* fruits as green inhibitor for C38 steel in hydrochloric acid solution

M. Manssouri[1], M. Znini[1], A. Ansari[1], A. Bouyenzer[2], Z. Faska[1] and L. Majidi[1]*

[1]Laboratoire des Substances Naturelles & Synthèse et Dynamique Moléculaire, Faculté des Sciences et Techniques, Errachidia, Morocco
[2]Laboratoire de Chimie Appliquée et Environnement, Faculté des Sciences, Oujda, Morocco

_____

ABSTRACT

The efficacy of the aqueous extracts of Ammodaucus leucotrichus fruits (E1 and E2) as corrosion inhibitors for C38 steel in 1M HCL solution has been studied by weight loss measurement as well as potentiodynamic polarization and electrochemical impedance spectroscopy (EIS) techniques. From loss measurements, is clear that inhibition efficiency values were significantly increased with increasing both concentration of each inhibitor and temperature. Polarization measurements showed that the studied inhibitors are mixed type with significant reduction of cathodic and anodic current densities. The results of EIS measurements indicated that the corrosion of steel is mainly controlled by the charge transfer process. Various activation and adsorption thermodynamic parameters are evaluated and discussed. Linearity of Langmuir isotherm adsorptions indicated the monolayer formation of each inhibitor on C38 steel surface.

Keywords: *Ammodaucus leucotrichus*, Aqueous extracts, Corrosion.
_____

INTRODUCTION

Carbon steel has wide spread industrial applications due to its availability and low cost compared with many metallic materials. In processes such acid cleaning, pickling, descaling and drilling operations in oil and gas exploration, acidic solutions are extensively used. However, acidic solutions cause corrosion of carbon steel [1]. In order to prevent unexpected metal dissolution and excess acid consumption in the process of cleaning, the use of inhibitors is one of the most practical methods for protection against corrosion [1,2].

Usually, organic compounds exert a significant influence on the extent of adsorption on the metal surface and therefore can be used as effective corrosion inhibitors. The efficiency of these inhibitors is related to the presence of polar functions with S, O or N atoms as well as conjugated double bonds or aromatic rings in their molecular structures which are the major adsorption centers usually regarded as the reaction center for the establishment of the adsorption process [3,4]. Although many of these compounds have high inhibition efficiencies, several are highly toxic to both human being and environment. Currently, research in corrosion is oriented to the development of "green corrosion inhibitors", compounds with good inhibition efficiency but low risk of environmental pollution [5,6]. The plant extracts have become important, as corrosion inhibitors, because they are environmentally acceptable, inexpensive, readily available and renewable sources of materials, and ecologically acceptable [7]. These extracts can be extracted by simple procedures with low cost and are biodegradable in the environment. Up till now, many plant extracts have been used as effective corrosion inhibitors for iron or steel in acidic media. For instance, the essential oils of *Mentha spicata*, *Lavandula multifida* and *Pulicaria mauritanica* [8-10] and the aqueous extract of Fenugreek (*Trigonella foenum graecum*) seeds and leaves [11], the aqueous extract of *Hibiscus sabdariffa* leaves [12], the aqueous extract of *Artemisia Halodendron* leaves [13] and the aqueous extract of Kalmegh (*Andrographis*

331

_____

paniculata) Leaves [14] have been test as corrosion inhibitors for metals. As a contribution to the current interest on environmentally friendly, green, corrosion inhibitors, the present study investigates the inhibiting effect of aqueous extract of *Ammodaucus leucotrichus* fruits.

Ammodaucus leucotrichus Coss. & Dur. (*Apiaceae* family) is the only one specie of the genus *Ammodaucus* [15]. It is a small annual plant (10-12 cm. high) with erect, finely striated stems. The leaves are finely dissected and slightly fleshy. The flowers with 5 free petals are grouped in umbels of 2 to 4 branches. The fruit (8-10 mm) is covered with dense silky white hairs. The plant has a strong smell of anise [15]. *A. leucotrichus* inhabits the maritime sands in the Saharan and sub-Saharan countries of North Africa, Morocco, Algeria and Tunisia, extending to Egypt and tropical Africa [16]. In Morocco, which locally known as "kammûn es-sofi or akâman", the fruits are used either by the local population as a powder or in a decoction to treat gastric-intestinal pain, gastralgias and indigestion [17]. It is also frequently used, as an infusion, for diverse infantile diseases of the digestive apparatus: dysentery, nausea, regurgitation, vomiting. Aqueous extracts of *A. leucotrichus* were shown to inhibit the formation of calcium oxalate monohydrate crystals and also found to potently inhibit the nucleation, growth and aggregation phases of calcium oxalate crystallization [18]. Antioxidant activities of the crude aqueous extracts of this plant were also reported [19]. The present work devotes to investigate the inhibitive effects of the aqueous extracts from the fruits of *A. leucotrichus* on corrosion of C38 steels in hydrochloric acid solution using weight loss, electrochemical polarization measurements and electrochemical impedance spectroscopy. The thermodynamic parameters were also obtained and discussed.

MATERIALS AND METHODS

Plant material and preparations of the aqueous extract (E1 and E2)
The *Ammodaucus leucotrichus* fruits were bought in a local market at Errachidia (Morocco). The botanical origin of samples was certified by the department of Biology of Faculty of Sciences and Technology of Errachidia (Morocco). A portion (100 g) of dried plant material was extracted with 1L of water under refluxing for 3 h. The liquid retentate was collected, filtered and centrifuged at 5000 rpm for 30 min. The supernatant was also filtered to eliminate any residues and lyophilized to give finally odorized aqueous extract (**E1**) in a yield of 9.37 % (w/w). However, the liquid retentate obtained after completion of hydrodistillation of 100 g dried plant material in 1L of water for 3 h, using a Clevenger-type apparatus to isolate volatile compounds, was collected, filtered, centrifuged and lyophilized to give finally deodorized aqueous extract (**E2**) in a yield of 5.82 % (w/w) [20].

Preparation of materials
C38 steel coupons containing 0.09 wt.% (P), 0.38 wt.% (Si), 0.01 wt.% (Al), 0.05 wt.% (Mn), 0.21 wt.% (C), 0.05 wt.% (S) and the remainder iron (Fe) used for weight loss measurements. The surface preparation of the C38 steel coupons (2 cm x 2 cm x 0.087 cm) was carried out with emery papers by increasing grades (400, 600 and 1200 grit size), then degreased with AR grade ethanol and dried at room temperature before use. The aggressive solutions of 1 M HCl was prepared by dilution of analytical grade 37% HCl with double distilled water. The concentration range of each inhibitor was 0.25-3 g/L. This concentration range was chosen upon the maximum solubility of E1 and E2. All reagents used for the study were of analytical grade.

Weight loss measurements
Weight loss tests were carried out in a double walled glass cell equipped with a thermostat-cooling condenser. The solution volume was 100 mL with and without the presence of different concentrations of E1 and E2 ranging from 0.25 to 3 g/L at various temperatures (308-343 K). After 6 h of immersion, the specimens of steel were carefully washed in double-distilled water, dried and then weighed. The rinse removed loose segments of the film of the corroded samples. Triplicate experiments were performed in each case and the mean value of the weight loss is reported using an analytical balance (precision $\pm$ 0.1 mg). Weight loss allowed us to calculate the mean corrosion rate as expressed in mg.cm^{-2} h^{-1}.
The corrosion rate (W_{corr}) and inhibition efficiency E_w (%) were calculated according to the Eqs. (1) and (2) respectively:

$$W = \frac{\Delta m}{St} \tag{1}$$

$$E_W \% = \frac{W_{corr} - W_{corr\,(inh)}}{W_{corr}} \times 100 \tag{2}$$

_____

where Δm (mg) is the specimen weight before and after immersion in the tested solution, W_{corr} and $W_{corr(inh)}$ are the values of corrosion weight losses (mg/cm^2.h) of C38 steel in uninhibited and inhibited solutions, respectively, S is the area of the C38 steel specimen (cm^2) and t is the exposure time (h).

The degree of surface coverage was calculated using:

$$\theta = \frac{W_{corr} - W_{corr\,(inh)}}{W_{corr}} \qquad (3)$$

where θ is surface coverage; $W_{corr\,(inh)}$ is corrosion rate for steel in presence of inhibitor, W_{corr} is corrosion rate for steel in the absence of inhibitor.

Electrochemical studies
Electrochemical measurements were carried out in a conventional three-electrode electrolysis cylindrical Pyrex glass cell. The working electrode (WE) in the form of disc cut from steel has a geometric area of 1 cm^2 and is embedded in polytetrafluoroethylene (PTFE). A saturated calomel electrode (SCE) and a disc platinum electrode were used respectively as reference and auxiliary electrodes, respectively. The temperature was thermostatically controlled at 308 K. The WE was abraded with silicon carbide paper (grade P1200), degreased with AR grade ethanol and acetone, and rinsed with double-distilled water before use.

Potentiodynamic polarization curves
Polarization curves studies were carried out using EG&G Instruments potentiostat-galvanosta (Model 263A) at 308 K without and with addition of various concentrations of E1 and E2 (0.25-3 g/L) in 1 M HCl solution at a scan rate of 0.5 mV/sec. Before recording the cathodic polarisation curves, the C38 steel electrode is polarised at -800 mV for 10 min. For anodic curves, the potential of the electrode is swept from its corrosion potential after 30 min at free corrosion potential, to more positive values. The test solution is deaerated with pure nitrogen. Gas bubbling is maintained through the experiments.

In the case of polarization method the relation determines the inhibition efficiency (E_I%):

$$E_I \% = \frac{I_{corr} - I_{corr(inh)}}{I_{corr}} \times 100 \qquad (4)$$

where I_{corr} and $I_{corr\,(inh)}$ are the corrosion current density values without and with the inhibitor, respectively, obtained by extrapolation of cathodic and anodic Tafel lines to the corrosion potential.

Electrochemical impedance spectroscopy (EIS)
The electrochemical impedance spectroscopy (EIS) measurements were carried out with the electrochemical system which included a digital potentiostat model Volta lab PGZ 100 computer at E_{corr} after immersion in solution without bubbling, the circular surface of C38 steel exposing of 1 cm^2 to the solution were used as working electrode. After the determination of steady-state current at a given potential, sine wave voltage (10 mV) peak to peak, at frequencies between 100 kHz and 10 mHz were superimposed on the rest potential. Computer programs automatically controlled the measurements performed at rest potentials after 30 min of exposure.

The impedance diagrams are given in the Nyquist representation. Values of R_t and C_{dl} were obtained from Nyquist plots. The charge-transfer resistance (R_t) values are calculated from the difference in impedance at lower and higher frequencies, as suggested by Tsuru et al. **[21]**. The inhibition efficiency got from the charge-transfer resistance is calculated by the following relation:

$$E_{Rt} \% = \frac{R'_t - R_t}{R'_t} \times 100 \qquad (5)$$

Where R_t and R'_t are the charge-transfer resistance values without and with inhibitor respectively. R_t is the diameter of the loop.

The double layer capacitance (C_{dl}) and the frequency at which the imaginary component of the impedance is maximal (-Z_{max}) are found determined by Eq. (6):

_____

$$C_{dl} = \frac{1}{\omega . R_t} \quad \text{where} \quad \omega = 2\,\pi\,.\,f_{max} \qquad (6)$$

Impedance diagrams are obtained for frequency range 100 KHz–10 mHz at the open circuit potential for C38 steel in 1 M HCl in the presence and absence of Aqueous extracts.

RESULTS AND DISCUSSION

Weight loss measurement
The non-electrochemical technique of weight loss was done in order to determine the corrosion rate (W) and percentage of inhibition (E_w) at various concentrations of Aqueous extracts and at different temperatures (Table 1).

Table 1: Corrosion Rate (W) and inhibition efficiency (E_w) of C38 steel in 1 M HCl in absence and presence of different concentrations of aqueous extract (E1 and E2) obtained from Weight Loss Measurements at different temperatures

	C (g/L)	308 K		313 K		323 K		333 K		343 K	
		W (mg/cm^2.h)	E_w (%)	W (mg/cm^2.h)	E_w (%)	W (mg/cm^2.h)	E_w (%)	W (mg/cm^2.h)	E_w (%)	W (mg/cm^2.h)	E_w (%)
	0	0.942	……..	1.751	……	2.836	……..	3.641	……	6.301	…….
E1	0.25	0.13	86.19	0.24	86.31	0.371	86.92	0.475	86.95	0.820	86.98
	1.00	0.102	89.17	0.186	89.38	0.294	89.63	0.369	89.86	0.607	90.36
	2.00	0.093	90.13	0.168	90.41	0.256	90.97	0.326	91.06	0.531	91.57
	3.00	0.053	94.39	0.094	94.61	0.148	94.78	0.189	94.81	0.325	**94.84**
E2	0.25	0.187	80.14	0.345	80.29	0.54	80.95	0.679	81.35	1.08	82.85
	1.00	0.167	82.27	0.3	82.86	0.482	83	0.618	83.02	1.009	83.98
	2.00	0.15	84.07	0.266	84.8	0.43	84.83	0.526	85.55	0.869	86.2
	3.00	0.093	90.12	0.17	90.29	0.254	91.04	0.349	90.41	0.514	**91.84**

The results indicated that the corrosion rate (W) of C38 steel decreased continuously with increasing the inhibitor concentration, ie, the corrosion of steel is retarded by each inhibitor, or the inhibition enhances with the inhibitor concentrations. This behavior is due to the fact that the adsorption coverage of inhibitor on steel surface increases with the inhibitor concentration. Also, the corrosion rate (W) increases with temperature both in uninhibited and inhibited solutions, especially goes up more rapidly in the absence of inhibitor. These results showed that E1 and E2 acts as an effective inhibitor in the range of temperature studied.

Moreover, the results reveal also that inhibition efficiency E_w increases sharply with increase in concentration of inhibitor, indicating that the extent of inhibition is dependent on the amount of E1 and E2 (concentration-dependent). At any given inhibitor concentration, the inhibition efficiency follows the order: E_w (E2) < E_w (E1), which indicates that E1 exhibits better inhibitive performance than E2. This difference in the inhibitory efficiency can be explained by the nature of the molecules of these inhibitors. Therefore, the effectiveness of E1 is due to the synergic effect of their volatile and non volatile compounds.

Also, we note that the efficiency (E_w) depends on the temperature and increases slightly with the rise of temperature from 308 to 343 K, and when the concentration reached to 3 g/L, the efficiency (E_w) reached a high values of 94.84 and 91.84 % in 1 M HCl solution at 343 K for E1 and E2, respectively, indicating the excellent inhibitive abilities of these inhibitors. The increase in inhibition efficiency with increase in temperature may be attributed to the increased adsorption of inhibitor molecules from metal surface and the inhibitory effect of inhibitor is reinforced at elevated temperature. Increase in inhibition efficiency with increasing inhibitor concentration and increased efficiency with increase in temperature is suggestive of chemical adsorption mechanism.

Potentiodynamic polarization curves
Potentiodynamic anodic and cathodic polarization plots for C38 steel specimens in 1 M HCl solution in the absence and presence of different concentrations of E1 and E2 at 308 K are shown in Figs. 1 and 2. The respective kinetic parameters including corrosion current density (I_{corr}), corrosion potential (E_{corr}), cathodic and anodic Tafel slopes (β_c, β_a) and inhibition efficiency (IE%) are given in Table 2.
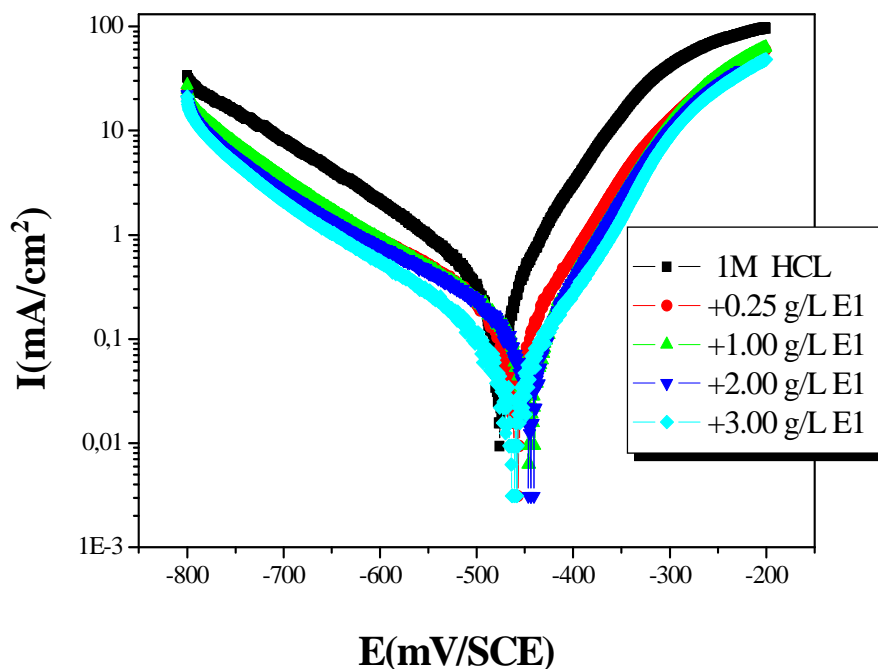
_____

Fig. 1. Anodic and cathodic polarization curves of C38 steel in 1 M HCl with various concentrations of E1
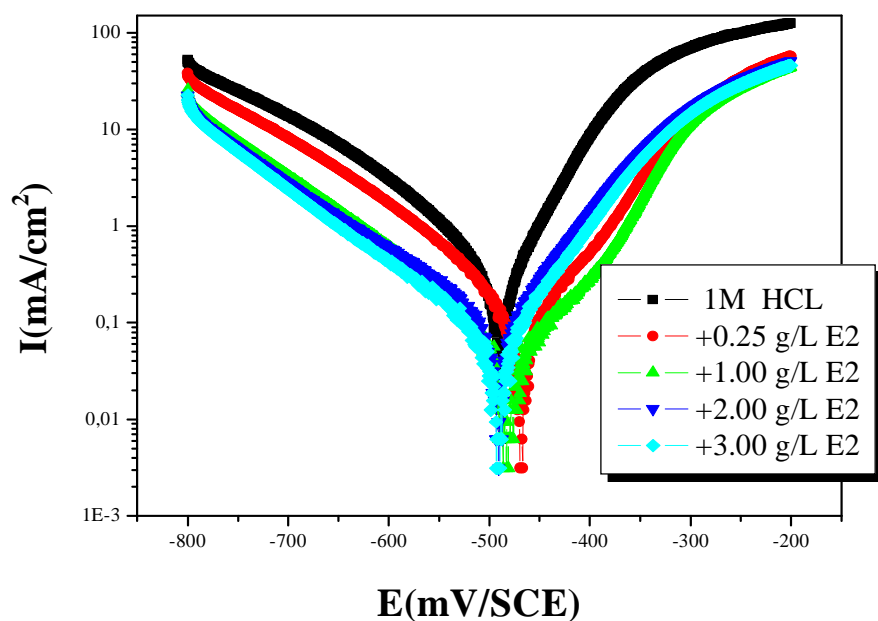

Fig. 2. Anodic and cathodic polarization curves of C38 steel in 1 M HCl with various concentrations of E2

Table 2 Polarization parameters for the C38 steel in 1 M HCl in absence and presence of various concentrations of aqueous extract from *A. leucotrichus* **fruits (E1and E2)**

	C (g/L)	- E_{corr} (mV/SCE)	I_{corr} (mA/cm²)	-β_c (mV)	β_a (mV)	IE%
	0	490.1	21.69	100	73.37	☐☐
E1	0.25	460.3	0.0857	100.9	66.4	85.17
	1.00	446.8	0.0778	104.4	64.1	86.53
	2.00	445.8	0.0701	109.2	62.9	87.86
	3.00	455.7	0.0518	99.09	60.7	**91.03**
E2	0.25	469.3	0.2211	145.3	92.2	61.74
	1.00	466.2	0.1019	142.2	80.1	82.37
	2.00	483.1	0.0803	134	84.7	86.1
	3.00	492.0	0.0573	128.7	72.7	**90.08**

Inspection of Figs. 1 and 2 shows that the addition of each inhibitor has an inhibitive effect in the both anodic and cathodic parts of the polarization curves. This indicates a modification of the mechanism of cathodic hydrogen evolution as well as anodic dissolution of steel, which suggest that each inhibitor powerfully inhibits the corrosion process of C38 steel, and its ability as corrosion inhibitor is enhanced as its concentration is increased. Further, the parallel cathodic Tafel curves in Figures 1 and 2 suggested that the hydrogen evolution is activation-controlled and the reduction mechanism is not affected by the presence of the inhibitor.

From Table 2, it is clear that increasing concentration of each inhibitor resulted in a decrease in corrosion current densities (I_{corr}) and an increase in inhibition efficiency (IE %), reaching its maximum value, 92.46 and 90.67 %, at 3 g/L for E1 and E2, respectively. This behavior suggests that the inhibitor adsorption protective film formed on the carbon steel surface tends to be more and more complete and stable. In addition, the fact that the slopes of the cathodic (β_c) and the anodic (β_a) Tafel lines are approximately constant with the addition of aqueous extracts indicates that these inhibitors act by simply blocking the available surface area. In other words, this result also indicates that the adsorbed molecules did not affect the mechanism of C38 steel dissolution or hydrogen evolution [22]. The presence of E1 and E2 caused a slight shift of corrosion potential towards the positive values compared to that in the absence of inhibitor. In literature, it has been also reported that if the displacement in E_{corr} is >85 mV the inhibitor can be seen as a cathodic or anodic type inhibitor and if the displacement of Ecorr is <85 mV, the inhibitor can be seen as mixed type [23]. In our study, the maximum displacement in E_{corr} value was 23.9 mV for E1 and 44.39 mV for E2 which indicates that the inhibitors acts as mixed type inhibitor with predominantly control of anodic reaction.

Electrochemical impedance spectroscopy (EIS)
The corrosion of C38 steel in 1 M HCl solution was investigated by EIS at 308 K after an exposure period of 30 min. Nyquist plots for C38 steel obtained at the interface in the absence and presence of different concentrations of inhibitors is given in Figs. 3 and 4.
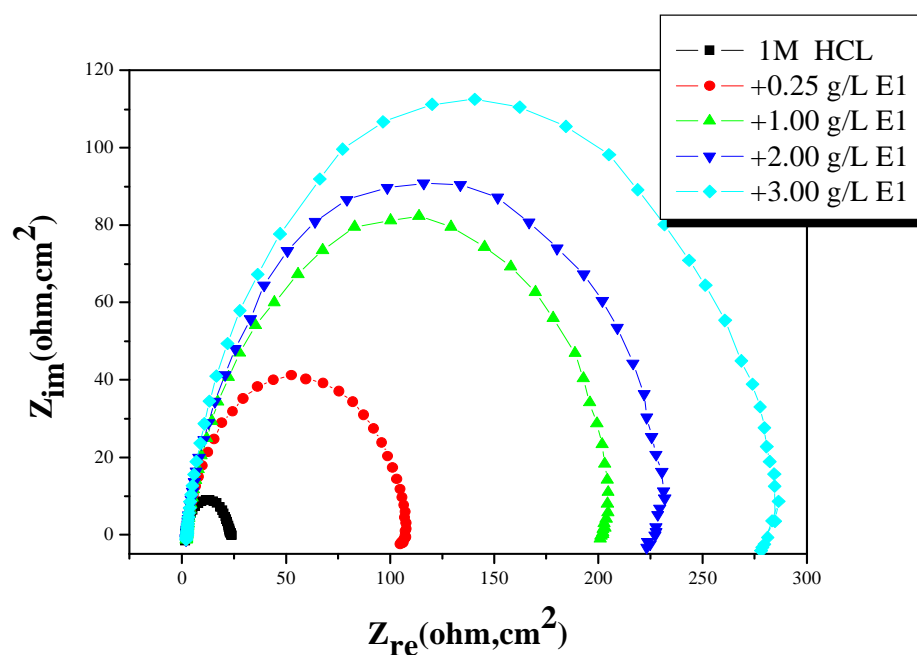

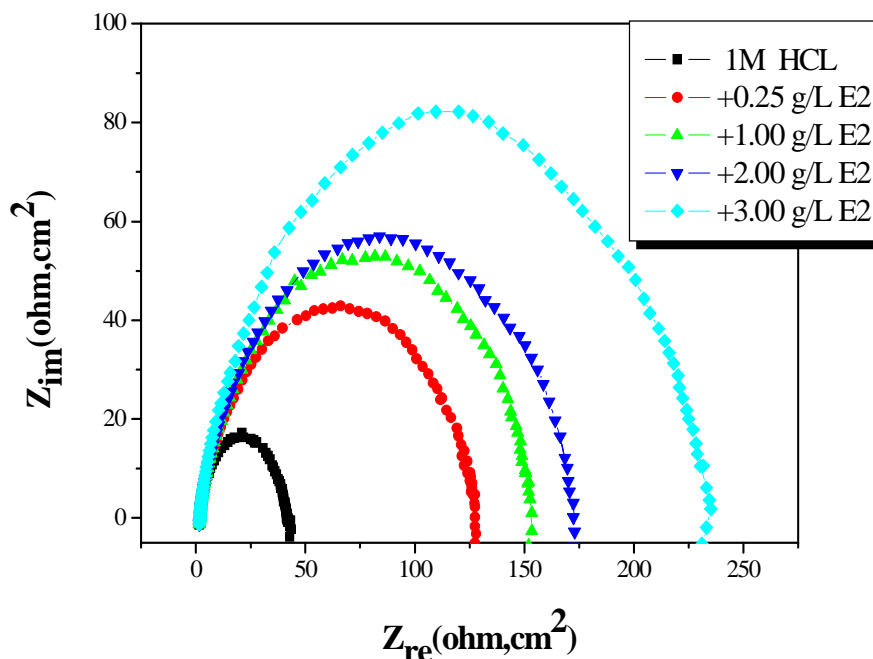**Fig. 3. Nyquist plots for C38 steel in 1 M HCl with various concentrations of E1**

_____

Fig. 4. Nyquist plots for C38 steel in 1 M HCl with various concentrations of E2

As shown in Figs 3 and 4, in uninhibited and inhibited 1 M HCl solutions, the impedance spectra exhibit one single capacitive loop, which indicates that the corrosion of steel is mainly controlled by the charge transfer process [24]. It is noted that these capacitive loops in 1 M HCl solutions are not perfect semicircles which can be attributed to the frequency dispersion effect as a result of the roughness and inhomogeneous of electrode surface [25]. Furthermore, the diameter of the capacitive loop in the presence of each inhibitor is larger than that in blank solution, and enlarges with the inhibitor concentration. This indicates that the impedance of inhibited substrate increases with the inhibitor concentrations, and leads to good inhibitive performance.

The electrochemical parameters of R_t, C_{dl} and f_{max} derived from Nyquist plots and inhibition efficiency E_{Rt} (%) are calculated and listed in Table 3.

Table 3 Electrochemical parameters for C38 steel in 1 M HCl with various concentrations of aqueous extracts E1 and E2

	C (g/L)	- E_{corr} (mV/SCE)	R_t ($\Omega.cm^2$)	f_{max} (H_Z)	C_{dl} ($\mu F.cm^2$)	E_{Rt}%
	0	490.1	21.69	100	73.37	--
E1	0.25	469.3	105.6	31.64	47.63	86.46
	1.00	466.2	197.2	20	40.35	89
	2.00	483.1	218.2	20	36.46	90.05
	3.00	492.0	287.6	20	27.66	**92.46**
E2	0.25	460.3	128.27	25	52.52	83.09
	1.00	446.8	168.94	25	46.46	87.16
	2.00	445.8	179.52	25	41.39	87.92
	3.00	455.7	232.41	25	40.24	**90.67**

It is apparent from Table 3 that the R_t values increase with inhibitor concentration and consequently the inhibition efficiency (E_{Rt}) increases to 92.46 and 90.67 % at 3 g/L for E1 and E2, respectively. In fact, the presence of inhibitors is accompanied by the increase of the value of R_t in acidic solution confirming a charge transfer process mainly controlling the corrosion of C38 steel. At any given inhibitor concentration, the inhibition efficiency follows the order: E_{Rt} (E2) < E_{Rt} (E1), which indicates that E1 exhibits better inhibitive performance than E2. Values of double layer capacitance are also brought down to the maximum extent in the presence of each inhibitor (27.66 and 40.24 $\mu F.cm^2$ at 3 g/L for E1 and E2, respectively) and the decrease in the values of C_{dl} follows the order similar to that obtained for I_{corr} in this study. The decrease in C_{dl} is due to the adsorption of the aqueous extracts on the metal surface leading to the formation of film or complex from acidic solution [26].

Moreover, the EIS results of these capacitive loops are simulated by the equivalent circuit shown in Fig. 5 to pure electric models that could verify or rule out mechanistic models and enable the calculation of numerical values corresponding to the physical and/or chemical properties of the electrochemical system under investigation [27]. In

_____

the electrical equivalent circuit, R_s is the electrolyte resistance, R_t the charge transfer resistance and C_{dl} is the double layer capacitance.
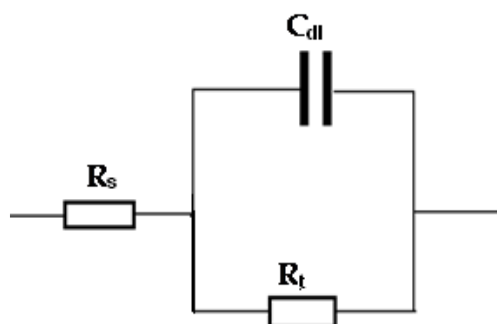

Fig. 5. Equivalent circuit used to fit the EIS data of C38 steel in 1 M HCl without and with different concentrations of aqueous extract from *A. leucotrichus* fruits (E1 and E2)

Moreover, the variation of inhibition efficiency (E %), determined by the three methods (weight loss, polarization curves and EIS methods), as a function of concentration of each inhibitor in 1 M HCl show a good agreement with the three methods used in this investigation.

Kinetic/Activation parameters
In order to calculate activation parameters of the corrosion reaction such as activation energy E°a, activated entropy ΔS°a and activation enthalpy ΔH°a for the corrosion of C38 steel in acid solution in absence and presence of different concentrations of inhibitors, the Arrhenius equation (7) and its alternative formulation called transition state equation (8) were employed **[28]**.

$$W = A\exp(-\frac{E^\circ_a}{RT}) \qquad (7)$$

$$W = \frac{RT}{Nh}\exp(\frac{\Delta S^\circ_a}{R})\exp(-\frac{\Delta H^\circ_a}{RT}) \qquad (8)$$

where E°a is the apparent activation corrosion energy, T is the absolute temperature, R is the universal gas constant, A is the Arrhenius pre-exponential factor, h is he Plank's constant, N is the Avogrado's number, ΔS°a is the entropy of activation and ΔH°a is the enthalpy of activation.
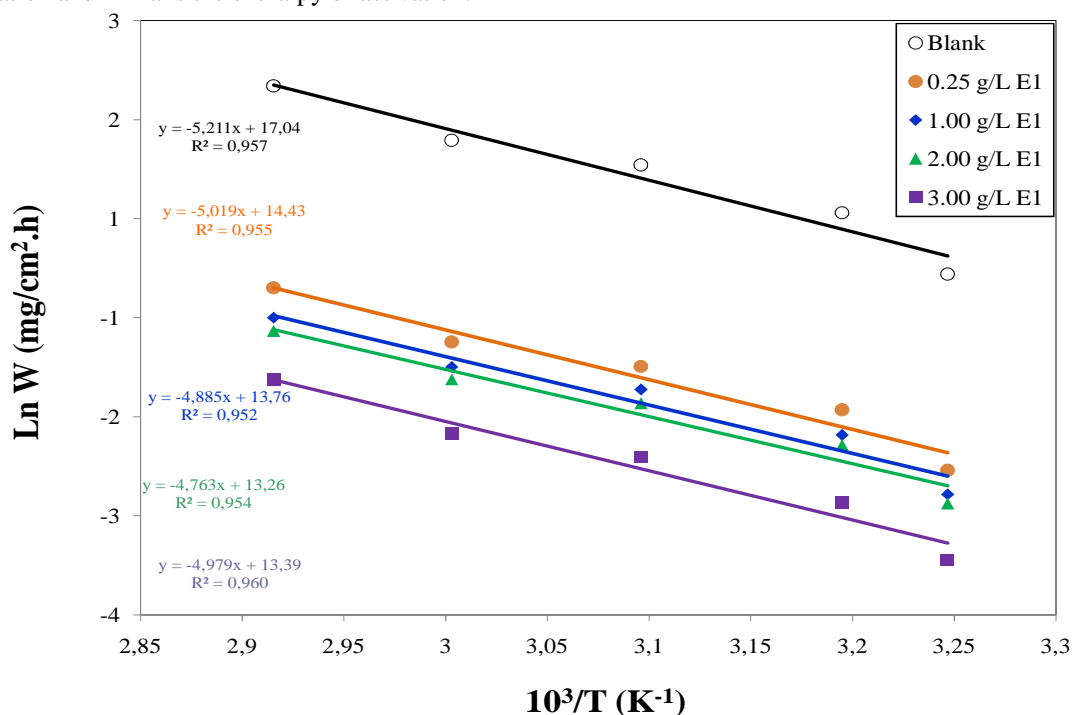

Fig. 6. Arrhenius plots for C38 steel corrosion rates (W) in 1 M HCl without and with different concentrations of E1
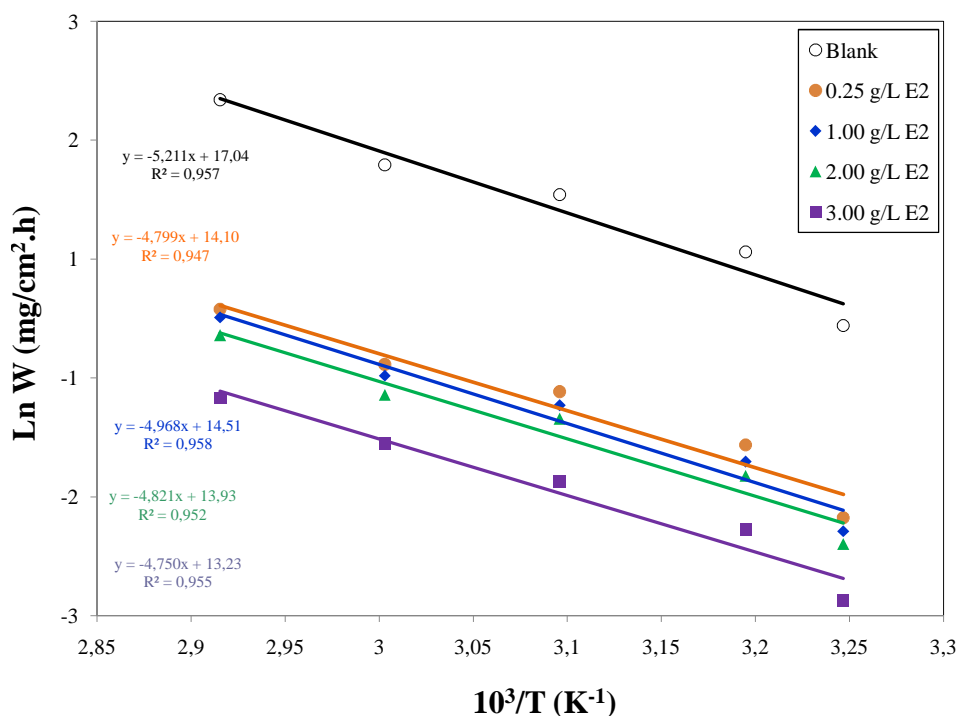
338

_____

Fig. 7. Arrhenius plots for C38 steel corrosion rates (W) in 1 M HCl without and with different concentrations of E2

Plotting the logarithm of the corrosion rate (W) versus reciprocal of absolute temperature, the activation energy can be calculated from the slope (-E°a/R). Figures 6 and 7 shows the variations of the logarithm of the corrosion rate (Ln W) versus reciprocal of absolute temperature (10^3/T) with the presence and absence of each inhibitor. The activation energy (E°a) values were calculated from the slope (-E°a/R) and the results are shown in Table 4. Further, using Eq. (8), plots of Ln (W/T) versus 10^3/T gave straight lines (Figures 8 and 9) with a slope of (-ΔH°a/R) and an intercept of (Ln(R/Nh) + (ΔS°a/R)) from which the values of ΔH°a and ΔS°a were calculated and are listed in Table 4.

The logarithm of the corrosion rate of steel Ln (W) can be represented as straight-lines function of (10^3/T) with the linear regression coefficient (R^2) was close to 1, indicating that the corrosion of steel in hydrochloric acid without and with inhibitor follows the Arrhenius equation.
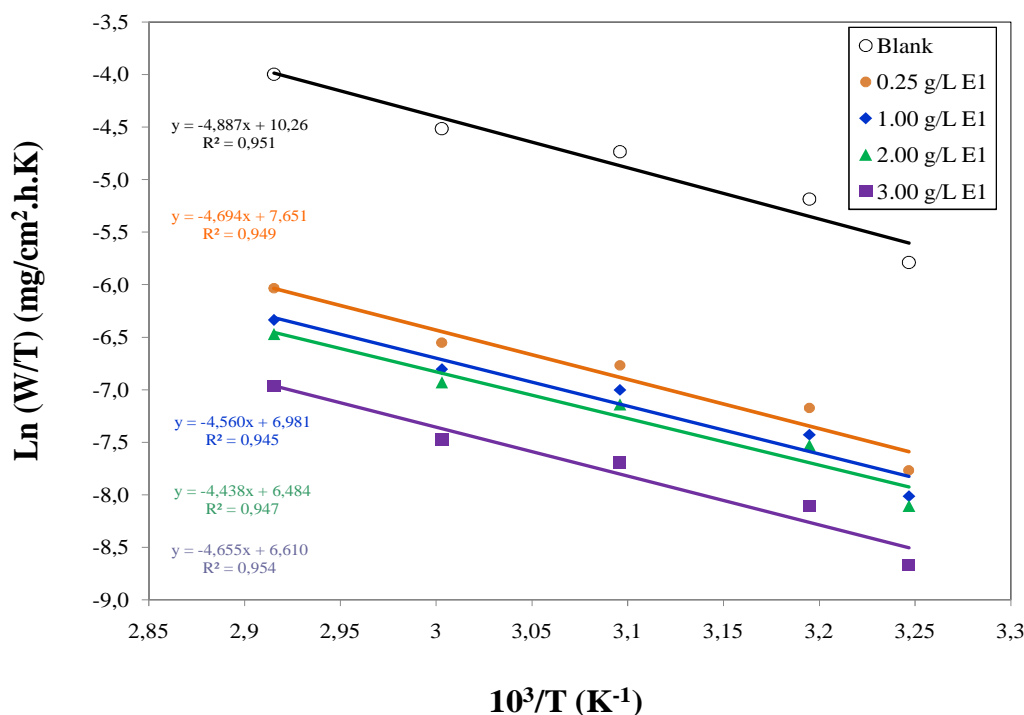

Fig. 8. Transition-state plot for C38 steel corrosion rates (W) in 1 M HCl without and with different concentrations of E1
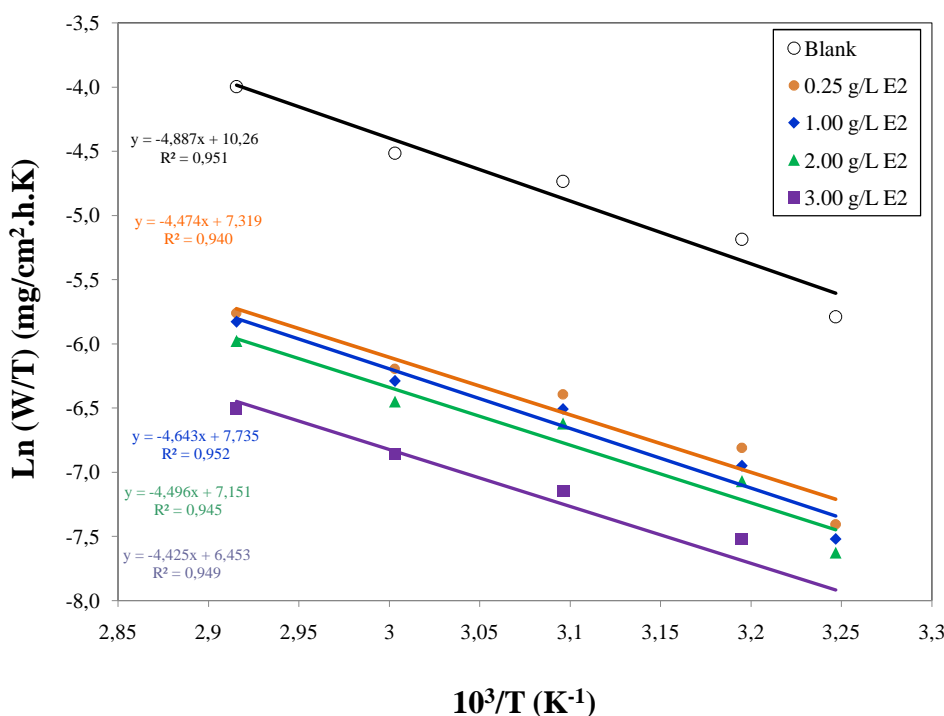
339

_____

Fig. 9. Transition-state plot for C38 steel corrosion rates (W) in 1 M HCl without and with different concentrations of E2

Table 4 Activation parameters E°a, ΔS°a, ΔH°a of the dissolution of C38 steel in 1 M HCl without and with different concentrations of E1 and E2

Inhibitor	C (g/L)	E°a (KJ. mol^{-1})	ΔH°a (KJ.mol^{-1})	E°a–ΔH°a (KJ. mol^{-1})	ΔS°a (J. mol^{-1}.K^{-1})
	0	43.35	40.65	2.70	-112.32
E1	0.25	41.76	38.67	2.70	-134.03
	1.00	40.64	37.94	2.70	-139.60
	2.00	39.63	36.92	2.71	-143.74
	3.00	41.42	38.72	2.70	-142.69
E2	0.25	39.93	37.22	2.71	-136.79
	1.00	41.33	37.13	2.70	-133.33
	2.00	40.11	37.41	2.70	-138.19
	3.00	39.52	36.82	2.70	-144.00

It is evident that the addition of the studied inhibitors affects the values of E°a; these values were observed lower than those in uninhibited acid solution (Table 4). This results show that the addition of each inhibitor decreases metal dissolution in 1 M HCl medium. In addition, the increase of E_w (%) with temperature is explained by a specific interaction between the steel surface and the inhibitor. Generally, the increase of E_w and the lower value of E°a of the corrosion process in an inhibitor's presence when compared to that in its absence is attributed to its chemisorption on the steel surface, while the opposite is the case with physical adsorption **[29].**
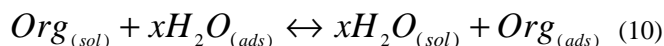
Also, the inspection of the data of table 4 reveals that the activation parameters (ΔH°a and ΔS°a) of the dissolution reaction of steel in 1 M HCl in the presence of the inhibitors were less than those in uninhibited acid solution (blank). The positive value of enthalpy of activation (ΔH°a) in the absence and presence of various concentration of inhibitors reflects the endothermic nature of C38 steel dissolution process meaning that dissolution of steel is difficult **[30]**. The negative values of entropies of activation (ΔS°a) imply that the activated complex in the rate determining step represents an association rather than a dissociation step, meaning that a decrease in disordering takes place on going from reactants to the activated complex **[31]**.

On the other hand, the average difference value of the E°a–ΔH°a is 2.7 KJ.mol^{-1}, which is approximately equal to the average value of RT (2.69 KJ.mol^{-1}) at the average temperature (323 K) of the domain studied. This result agrees that the corrosion process is a unimolecular reaction as described by the known Eq. (9) of perfect gas:

$$E°a – ΔH°a = RT \qquad\qquad (9)$$

_____

Adsorption isotherm and thermodynamic parameters

It is know that the adsorption process of inhibitor depends on its electronic characteristics, the nature of metal surface, temperature, steric effects and the varying degrees of surface-site activity. In fact, the solvent H_2O molecules could also be adsorbed at the metal/solution interface. In the aqueous solution, the adsorption of inhibitor molecules can be considered as a quasi-substitution process between the inhibitor in the aqueous phase $Inh_{(sol)}$ and water molecules at the electrode surface $H_2O_{(ads)}$ [32]:

$$Org_{(sol)} + xH_2O_{(ads)} \leftrightarrow xH_2O_{(sol)} + Org_{(ads)} \quad (10)$$

where x is the size ratio, that is, the number of water molecules re-placed by one organic inhibitor.

This equation showed that the interaction force between metal and inhibitor must be greater than the interaction force of metal and water molecule. The character of adsorption of inhibitor in combination with halides was elucidated from the degree of surface coverage (θ) values calculated from the weight loss data ($\theta = E_w/100$) at different temperatures. The values of surface coverage, θ for the inhibitor have been used to explain the best isotherm to determine the adsorption process. Attempts were made to fit θ values to various adsorption isotherms namely Frumkin, Temkin. Langmuir and Freundlich.

It was assumed that the adsorption of E1 and E2 would follow the Langmuir adsorption isotherm. The plot of C/θ versus C (Figs. 10 and 11) yields a straight line with all linear correlation coefficients (R^2) are almost equal to 1, and the slope values are also close to 1, supporting the assumption that the adsorption of each inhibitor from hydrochloric acid solution on the C38 steel surface obeys a Langmuir adsorption isotherm, which is represented by Eq. (11). This result showed that the adsorbed molecules occupy only one site and there are no interactions with other adsorbed species [33].

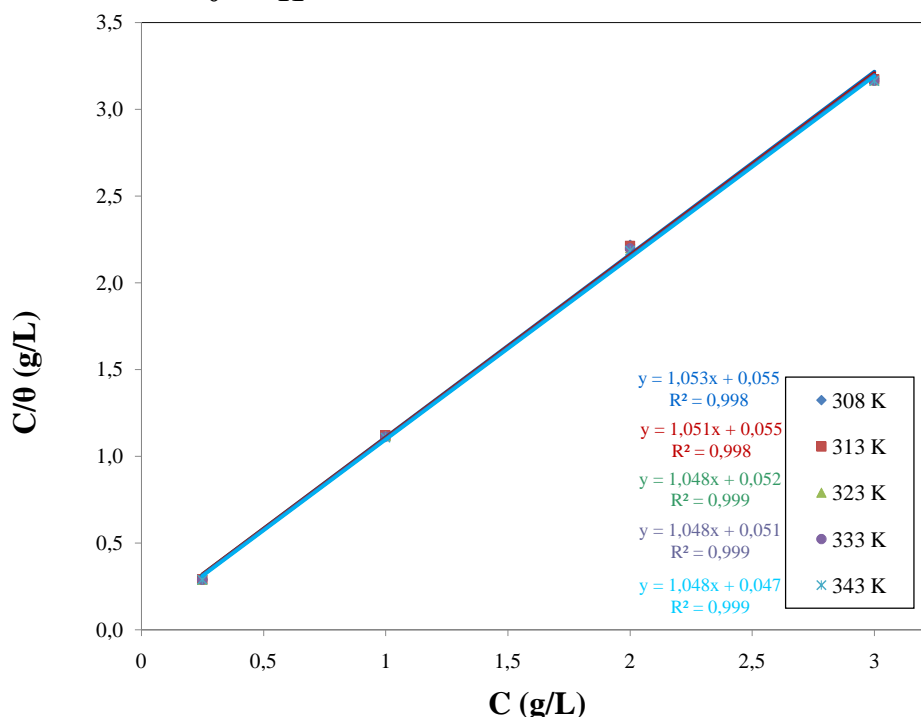$$\frac{C}{\theta} = \frac{1}{K} + C \quad (11)$$

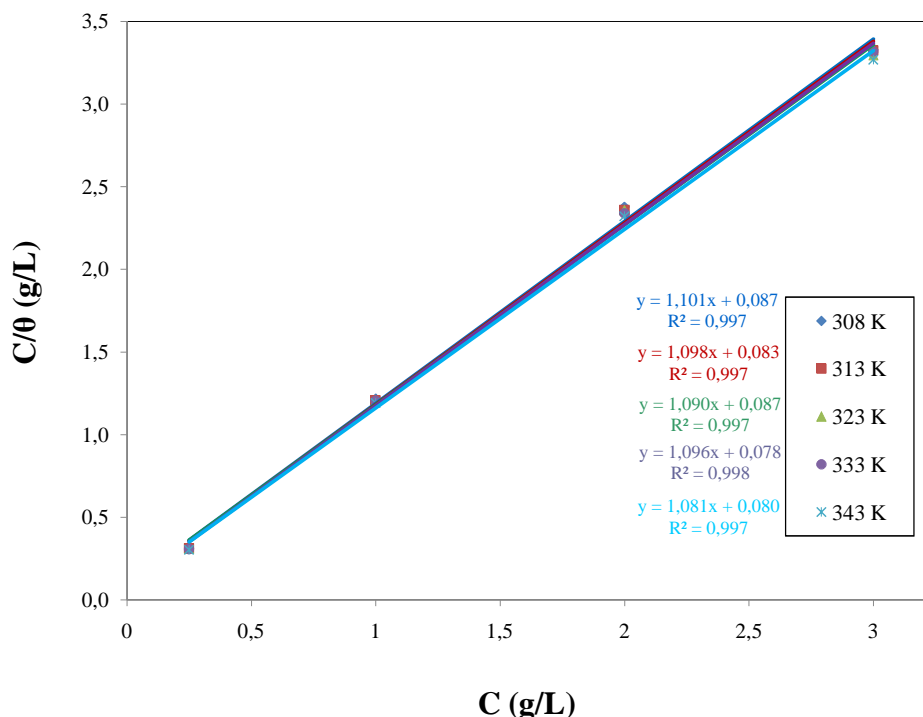**Fig. 10. Langmuir adsorption isotherm of E1 on the C38 steel surface in 1 M HCl**

_____

Fig. 11. Langmuir adsorption isotherm of E2 on the C38 steel surface in 1 M HCl

Thermodynamic parameters are important to further understand the adsorption process of inhibitor on steel/solution interface. The equilibrium adsorption constant, K is related to the standard Gibb's free energy of adsorption (ΔG°_{ads}) with the following equation:

$$K = \frac{1}{55.5}.\exp\left(-\frac{\Delta G^{\circ}_{ads}}{RT}\right) \tag{12}$$

The standard adsorption enthalpy (ΔH°_{ads}) could be calculated on the basis of Van't Hoff equation [34]:

$$LnK = -\frac{\Delta H^{\circ}_{ads}}{RT} + D \tag{13}$$

where R is the universal gas constant, T is the thermodynamic temperature, D is integration constant, and the value of 55.5 is the concentration of water in the solution in mol/L (10^3 g/L).

The standard adsorption enthalpy (ΔH°_{ads}) can also be calculated from the Gibbs-Helmholtz equation:

$$\frac{\Delta G^{\circ}_{ads}}{T} = \frac{\Delta H^{\circ}_{ads}}{T} + k \tag{14}$$

To calculate the enthalpy of adsorption (ΔH°_{ads}), LnK was plotted against 1/T (Fig. 12) and straight line was obtained with slope equal to ($-\Delta H^{\circ}_{ads}/R$). Also, the variation of $\Delta G^{\circ}_{ads}/T$ vs 1/T gives straight line with slope equal to ΔH°_{ads} (Fig. 13).

With the obtained both parameters of ΔG°_{ads} and ΔH°_{ads}, the standard adsorption entropy (ΔS°_{ads}) can be calculated using the following thermodynamic basic Equ. (13). All the standard thermodynamic parameters are listed in Table 5.

$$\Delta S^{\circ}_{ads} = \frac{\Delta H^{\circ}_{ads} - \Delta G^{\circ}_{ads}}{T} \tag{15}$$

_____

Table 5 Thermodynamic parameters for adsorption of E1 and E2 on C38 steel in 1 M HCl solution at different temperatures from Langmuir adsorption isotherm

Inhibitor	T (K)	R^2	K (L/g)	$\Delta G°_{ads}$ (KJ.mol^{-1})	$\Delta H°_{ads}$	(KJ. mol^{-1})	$\Delta S°_{ads}$ (J.mol^{-1}.K^{-1})
E1	308	0.998	18.18	-25,13			124,75
	313	0.998	18.18	-25,54	13.21 Eq (13)		125,03
	323	0.999	19.23	-26,51	13.21 Eq (14)		126,58
	333	0.999	19.60	-27,38			125,63
	343	0.999	21.28	-28,44			124,52
E2	308	0.997	11.49	-23,96			84,94
	313	0.997	12.05	-24,47	2.205 Eq (13)		85,23
	323	0.997	11.49	-25,12	2.207 Eq (14)		84,61
	333	0.998	12.82	-26,21			85,32
	343	0.997	12.50	-26,92			84,92

Data in Table 5 revealed that the adsorptive equilibrium constant (K) increased with increasing temperature, which indicated that the inhibitors were easily and strongly adsorbed onto the C38 steel surface at relatively higher temperature. This could be due to formation of coordinated bond between the prepared aqueous extracts and the d-orbital of iron on the surface of steel through lone pair of electron of hetero atoms [35].

The negative values of $\Delta G°_{ads}$ suggest that the adsorption of inhibitor molecules onto steel surface is a spontaneous phenomenon. It is well known that values of $\Delta G°_{ads}$ around –20 KJ.mol^{-1} or lower are associated with the physiosorption phenomenon where the electrostatic interaction assemble between the charged molecule and the charged metal, while those around –40 KJ.mol^{-1} or higher are associated with the chemiosorption phenomenon where the sharing or transfer of organic molecules charge with the metal surface occurs [36]. In the present study, the value of $\Delta G°_{ads}$ computed and shown in Table 5 were about -23.96 to -28.44 KJ.mol^{-1}; which may be due to mixture physical and chemical adsorption of each inhibitor on C38 steel surface [36].

Also, the positives values of $\Delta H°_{ads}$ mean that the dissolution process is an endothermic phenomenon which indicates that, the inhibition efficiency increases with the temperature increasing [37]. Such behavior can be interpreted on the basis that the increase in temperature resulted in sorption of inhibitor molecules on the metal surface. In addition, the value of the enthalpy of adsorption found by the two methods such as Van't Hoff (Eq (13)) and Gibbs–Helmholtz relations (Eq (14)) are in good agreement.

Moreover, the positive value of $\Delta S°_{ads}$ in the presence of inhibitor is an indication of increase in solvent entropy. This increase of entropy was the driving force of the adsorption of inhibitor onto carbon steel surface [38]. Also, the positive value of $\Delta S°_{ads}$ since the endothermic adsorption process is always accompanied by an increase of entropy.

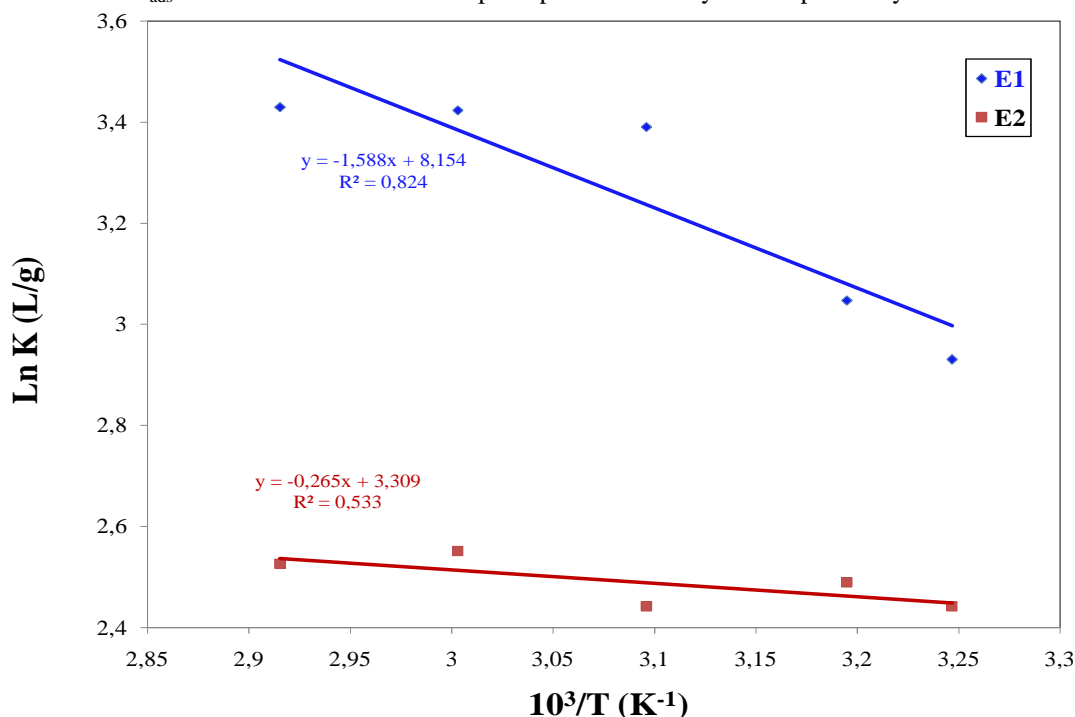**Fig. 12. Van't Hoff's plot of Ln K against 1/T for the adsorption of E1 and E2 onto C38 steel**
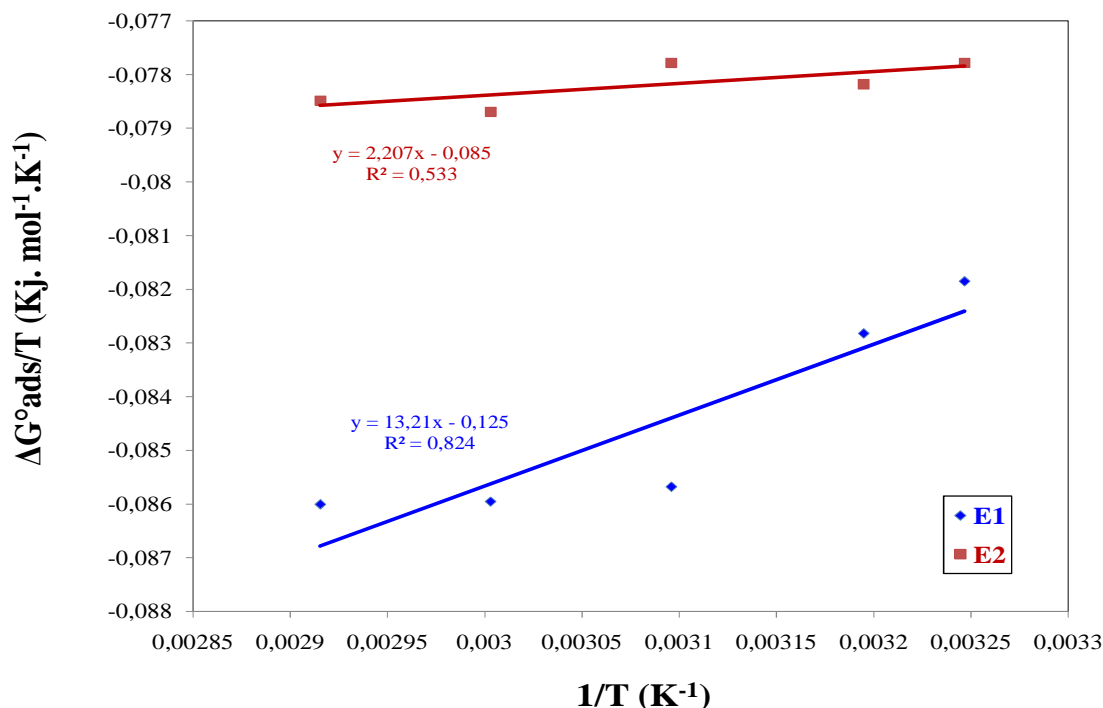
343

_____

Fig. 13. The relationship between (ΔG°ads/T) and 1/T of E1 and E2

Explanation for inhibition

The inhibition mechanism involves the adsorption of the inhibitor on the metal surface immersed in aqueous HCl solution. Four types of adsorption **[39]** may take place involving organic molecules at the metal–solution interface: electrostatic attraction between the charged molecules and the charged metal; interaction of unshared electron pairs in the molecule with the metal; interaction of π-electrons with the metal; and a combination of all the above.

The predominant adsorption mode of E1 and E2 depends upon factors such as the nature of the extract molecules, type of acid anion, as well as chemical changes in the extracts. Molecule adsorption of the E1 and E2 at the metal surface can be attributed to the presence of electronegative elements such as oxygen and nitrogen atoms and also to the presence of π-electrons. The high inhibitive performance of E1 is due to the synergic effect of their volatile and non volatile compounds.

In general, there are two ways to explain the inhibition of the dissolution reaction by adsorption at the metal surface **[40]**. In acid solution, the protonation of the aqueous extracts may occur easily, so it is difficult for the protonated extracts to approach the positively charged carbon steel surface (H_3O^+/metal interface) due to the electrostatic repulsion. Since chloride ions have a smaller degree of hydration, thus they could bring excess negative charges in the vicinity of the interface and favour more adsorption of the positively charged inhibitor molecules, the protonated fruits extracts adsorbed through electrostatic interactions between the positively charged molecules and the negatively charged metal surface. Another way to explain the inhibition involves the donation of lone pairs of electrons to the surface and the interaction of π-electrons of the aromatic/heterocyclic ring with the metal surface, which may be the main role. The two ways can influence in the inhibition corrosion in cooperative mode.

CONCLUSION

The inhibition efficiency of aqueous extracts of *A. leucotrichus* fruit (E1 and E2) on corrosion of C38 steel in 1 M HCl was examined by weight loss and electrochemical measurement. The aqueous extracts of *A. leucotrichus* fruit showed significant corrosion inhibition activity. The results obtained from the weight loss measurements were in good agreement with those obtained from the potentiodynamic polarization and EIS methods. From weight loss measurements, the inhibition efficiency value increases with the increasing of inhibitor concentrations and temperature. Polarization curves indicated that each inhibitor acts as a mixed type inhibitor in 1 M HCl. The inhibition is accomplished by a mixture physical and chemical adsorption of the extract components on the steel surface leading to a reduction in the double layer capacitance as well as an increase in the charge transfer resistance. The adsorption of E1 and E2 is spontaneous and obeys the Langmuir isotherm.

_____

REFERENCES

[1] N.A. Odewunmi, S.A. Umoren, Z.M. Gasem, *J. Ind. Eng. Chem*., **2014**; http://dx.doi.org/10.1016/j.jiec.**2014**.02.030.

[2] A.A. Farag, T.A. Ali, J. Ind. Eng., **2014**; http://dx.doi.org/10.1016/j.jiec.**2014**.03.030.

[3] P.R. Roberge, Handbook of Corrosion Engineering, McGraw-Hill., New York, **1999**.

[4] O. Benali, L. Larabi, S.M. Mekelleche, Y. Harek, *J. Mater. Sci*., **2006**, 41, 7064.

[5] M.K. Pavithra, T.V. Venkatesha, M.K. Punith Kumar, H.C. Tondan, *Corros. Sci*., **2012**, 60, 104.

[6] H. Cang, Z.H. Fei, J.L. Shao, W.Y. Shi, Q. Xu, *Int. J. Electrochem. Sci*., **2013**, 8, 720.

[7] N. Soltani, N. Tavakkoli, M.K. Kashani, A. Mosavizadeh, E.E. Oguzie, M.R. Jalali, *J. Ind. Eng. Chem*., **2014**; http://dx.doi.org/10.1016/j.jiec.**2013**.12.002.

[8] M. Znini, M. Bouklah, L. Majidi, S. Kharchouf, A. Aouniti, A. Bouyanzer, B. Hammouti, J. Costa, S.S. Al-Deyab, *Int. J. Electrochem. Sci.,* **2011**, 6, 691.

[9] M. Znini, J. Paolini, L. Majidi, J.M. Desjobert, J. Costa, N. Lahhit, A. Bouyanzer*, Res. Chem. Intermed*., **2012**, 38, 669.

[10] G. Cristofari, M. Znini, L. Majidi, A. Bouyanzer, S.S. Al-Deyab, J. Paolini, B. Hammouti, J. Costa, *Int. J. Electrochem. Sci.,* **2011**, 6, 6699.

[11] E.A. Noor, *J. Eng. Applied. Sci*., **2008**, 3, 23-30.

[12] E.A. Noor, *J. Appl. Electrochem*., **2009**, 39, 1465-1475.

[13] J. Huang, H. Cang, Q. Liu, J. Shao, *J. Electrochem. Sci*., **2011**, 8, 8592-8602.

[14] A. Singh, V.K. Singh, M.A. Quraishi, Int. J. Corros., **2010**; http://dx.doi.org/10.1155/**2010**/27598

[15] P. Ozenda, Flore et Végétation du Sahara, CNRS, Paris (**1991**), 3ème Ed, p. 360.

[16] P.L. Maberly, The Plant Book, Cambridge University Press, Cambridge, **1998**.

[17] J. Bellakhdar, La pharmacopée marocaine traditionnelle. Médecine arabe ancienne et savoirs populaires. IBIS Press, (**1997**), p. 764.

[18] M. Beghali, S. Ghalem, H. Allali, A. Belouatek, A. Marouf Malay, *J. Biochem . Mol. Biol*., **2008**, 16 , 11.

[19] W. Rached, H. Benamar, M. Bennaceur, A. Marouf, *J. Biol.* Sci., **2010**, 10, 316.

[20] A. Dapkevicius, R. Venskutonis, T.A. Van Beek, P.H. Linssen, *J. Sci. Food Agric*., **1998**, 77, 140-146.

[21] T. Tsuru, S. Haruyama, B. Gijutsu, *Japan Society* of *Corrosion Engineering* 27, (**1978**), 573.

[22] E.S. Ferreira, C. Giacomelli, F.C. Giacomelli, A. Spinelli, *Mater. Chem. Phys*., **2004**, 83, 129-134.

[23] A.K. Satapathy, G. Gunasekaran, S.C. Sahoo, K. Amit, P.V. Rodrigues, *Corros. Sci*., **2009**, 51, 2848.

[24] A.R. Sathiyapriya, V.S. Muralidharan, A. Subramanian, *Corros*., **2008**, 64, 541.

[25] F. Mansfeld, M.W. Kendig, S. Tsai, *Corros*., **1982**, 38, 570.

[26] M. Lagrenée, B. Mernari, M. Bouanis, M. Traisnel, F. Bentiss, *Corros. Sci*., **2002**, 44, 573.

[27] M. Benabdellah, A. Aouniti, A. Dafali, B. Hammouti, M. Benkaddour, A. Yahyi, A. Ettouhami, *Appl. Surf. Sci.,* **2006**, 252, 8341-8347.

[28] F. Mansfeld, M.W. Kendig, S. Tsai, *Corros*., **1982**, 38, 570.

[29] A.M. Badiea, K.N. Mohana, *Corros. Sci.,* **2009**, 51, 2231-2241.

[30] E. Khamis, F. Bellucci, R. Latanision, E.S. El Ashry, *Corros*., **1991**, 47, 677-686.

[31] F. Bentiss, M. Lebrini, H. Vezin, F. Chai, M. Traisnel, M. Lagrené, *Corros. Sci*., **2009**, 51, 2165-2173.

[32] I. El Ouali, B. Hammouti, A. Aouniti, Y. Ramli, A. Azougagh, E. Essassi, M. Bouachrine, *J. Mater.* Env. Sci., **2010**, 1, 1.

[33] S. Cheng, S. Chen, T. Liu, X. Chang, Y. Yin, *Mater. Lett*., **2007**, 61, 3279.

[34] T. Libin, M. Guannan, L. Guangheng, *Corros. Sci.,* **2003**, 45, 2251.

[35] M.A. Hegazy, A.S. El Tabei, A.H. Bedair, M.A. Sadeq, *Corros. Sci.,* **2012**, 54, 219-230.

[36] F. Bentiss, M. Lebrini, H. Vezin, F. Chai, M. Traisnel, M. Lagrené, *Corros. Sci*., **2009**, 51, 2165-2173.

[37] M.A. Hegazy, H.M. Ahmed, A.S. El Tabei, *Corros. Sci.,* **2011**, 53, 671-678.

[38] G.N. Mu, X.H. Li, Q. Qu, J. Zhou, *Acta Chim. Sinica*., **2004**, 62, 2386-2394.

[39] D.P. Schweinsberg, A. Graeme, George, A.K. Nanayakkara, D.A. Steinert, *Corros. Sci*., **1988**, 28-33.

[40] F. Bentiss, M. Traisnel, M. Lagrenee, *J. Appl. Electrochem*., **2001**, 31-41.